Molecular Chromium(III)−Lanthanide(III) Compounds (Ln = La, Ce, Pr, Nd) with a Polymeric, Ladder-Type Architecture: A Structural and Magnetic Study

Silvio Decurtins,*,† Mathias Gross,† Helmut W. Schmalle,‡ and Sylvie Ferlay†

Departement für Chemie und Biochemie, Universität Bern, Freiestrasse 3, CH-3012 Bern, Switzerland, and Anorganisch-chemisches Institut, Universität Zürich, Winterthurerstrasse 190, CH-8057 Zürich, Switzerland

Received November 25, 1997

Reaction of tris(oxalato)chromium(III) complexes, $[Cr^{III}(ox)_3]^{3-}$ ($ox^{2-} = C_2O_4^{2-}$), with salts of the trivalent rare earth ions, Ln = La, Ce, Pr, and Nd, generates the polymeric 3d−4f coordination solids with stoichiometries $[Ln^{III}Cr^{III}(ox)_3(H_2O)_4]_2 \cdot nH_2O$, *n* varies from 12 to 7. Results of single-crystal structural analyses of two representative compounds within the isostructural series are discussed. Crystal data: $[La^{III}Cr^{III}(ox)_3(H_2O)_4]_2 \cdot 12H_2O$ (**1**), monoclinic, space group *C*2, $a = 36.080(8)$ Å, $b = 10.906(1)$ Å, $c = 10.935(2)$ Å, $\beta = 105.55(1)°$, $Z = 4$; $[Ce^{III}Cr^{III}(ox)_3(H_2O)_4]_2 \cdot 12H_2O$ (**2**), monoclinic, space group *C*2, $a = 36.075(6)$ Å, $b = 10.887(1)$ Å, $c = 10.913(2)$ Å, $\beta = 105.65(1)°$, $Z = 4$. X-ray powder diffraction established the isostructurality within the series, and from thermal gravimetry analyses, the number of water molecules of crystallization for the conditioned, polycrystalline samples was determined. The crystal structures assume extended molecular arrays based on two types of symmetrically independent molecular chains with a ladder-type motif. Therein, the metal ions are mutually bridged by three oxalate ligands; thus, the tris-chelated Cr(III) ion has a slightly distorted octahedral environment, whereas the tris-chelated Ln(III) ion is 10-coordinated with four additional water molecules in its coordination sphere. Two other compounds of the same stoichiometry, involving the Eu(III) and Tb(III) ions, are presented. A preliminary study of the magnetic properties of the structurally characterized compounds is reported.

Introduction

The spontaneous self-assembly of metal ions with a preference for a particular coordination geometry and of the appropriate connecting organic ligands leads in favorable cases to crystalline coordination solids showing specific molecular topologies and crystal packing motifs. While the rules of the various network topologies are still being learned, there has been a rapid development over the past few years in the phenomenological experience within these fascinating fields of supramolecular chemistry[1] and crystal engineering,[2] and a growing body of studies is continually enlarging our playing field.

A particular interesting topic within this context is the synthesis of heterometallic molecular assemblies comprising 3d-metal centers and 4f-metal centers, whereby the importance of the lanthanide metal ions mainly results from the peculiar spectroscopic and magnetic properties associated with their $4f^n$ electronic configurations.[3] Recently, many authors have reported on the syntheses and solid-state properties of heterodinuclear,[4−6] heteropolynuclear,[7−10] and polymeric[11−15] 3d−4f coordination compounds. Overall, the rich chemistry which is expressed through a diversity of bridging motifs and a range of metal ion to metal ion distances within the molecules has mainly been applied to the investigation of magnetic exchange interactions between the 3d and 4f metal centers. In particular, copper(II)−gadolinium(III) complexes have been especially significant since a distinct ferromagnetic coupling was first reported in 1985.[16]

While focusing our attention primarily on the structural aspects of the extended, polynuclear 3d−4f complexes, it is interesting to note that, as a distinctive structural feature, a

* To whom correspondence should be addressed.
† Universität Bern.
‡ Universität Zürich.

(1) Lehn, J. M. *Supramolecular Chemistry;* VCH Press: Weinheim, Germany, 1995.
(2) Desiraju, G. *R. Angew. Chem., Int. Ed. Engl.* **1995**, *34*, 2328.
(3) Bünzli, J.-C. G., Choppin, G. R., Eds. *Lanthanide Probes in Life, Chemical and Earth Sciences;* Elsevier: Amsterdam, 1989.
(4) (a) Costes, J.-P.; Dahan, F.; Dupuis, A.; Laurent, J.-P. *Inorg. Chem.* **1996**, *35*, 2400. (b) Costes, J.-P.; Dahan, F.; Dupuis, A.; Laurent, J.-P. *Inorg. Chem.* **1997**, *36*, 4284.
(5) Ramade, I.; Kahn, O.; Jeannin, Y.; Robert, F. *Inorg. Chem.* **1997**, *36*, 930.
(6) Piguet, C.; Rivara-Minten, E.; Bernardinelli, G.; Bünzli, J.-C. G.; Hopfgartner, G. *J. Chem. Soc., Dalton Trans.* **1997**, 421.
(7) Andruh, M.; Ramade, I.; Codjovi, E.; Guillou, O.; Kahn, O.; Trombe, J. C. *J. Am. Chem. Soc.* **1993**, *115*, 1822.
(8) Benelli, C.; Blake, A. J.; Milne, P. E. Y.; Rawson, J. M.; Winpenny, R. E. P. *Chem. Eur. J.* **1995**, *1*, 614.
(9) Chen, X.-M.; Aubin, S. M. J.; Wu, Y.-L.; Yang, Y.-S.; Mak, T. C. W.; Hendrickson, D. N. *J. Am. Chem. Soc.* **1995**, *117*, 9600.
(10) Brechin, E. K.; Harris, S. G.; Parsons, S.; Winpenny, R. E. P. *J. Chem. Soc., Dalton Trans.* **1997**, 1665.
(11) Deng, H.; Shore, S. G. *J. Am. Chem. Soc.* **1991**, *113*, 8538.
(12) Bouayad, A.; Brouca-Cabarrecq, C.; Trombe, J. C.; Gleizes, A. *Inorg. Chim. Acta* **1992**, *195*, 193.
(13) Knoeppel, D. W.; Shore, S. G. *Inorg. Chem.* **1996**, *35*, 5328.
(14) (a) Guillou, O.; Kahn, O.; Oushoorn, R. L.; Boubekeur, K.; Batail, P. *Inorg. Chim. Acta* **1992**, *198*, 119. (b) Guillou, O.; Bergerat., P.; Kahn, O.; Bakalbassis, E.; Boubekeur, K.; Batail, P.; Guillot, M. *Inorg. Chem.* **1992**, *31*, 110. (c) Oushoorn, R. L.; Boubekeur, K.; Batail, P.; Gouillou, O.; Kahn, O. *Bull. Soc. Chim. Fr.* **1996**, *133*, 777.
(15) (a) Hulliger, F.; Landolt, M.; Vetsch, H. *J. Solid State Chem.* **1976**, *18*, 283. (b) Hulliger, F.; Landolt, M.; Vetsch, H. *J. Solid State Chem.* **1976**, *18*, 307. (c) Xu, X.-L.; Emmenegger, R.; Hulliger, F. *J. Solid State Inorg. Chem.* **1990**, *27*, 537. (d) Hulliger, F.; Vetsch, H.; Xu, X.-L. *J. Solid State Inorg. Chem.* **1995**, *32*, 907. (e) Hulliger, F.; Vetsch, H. *J. Solid State Inorg. Chem.* **1996**, *33*, 33.
(16) Bencini, A.; Benelli, C.; Caneschi, A.; Carlin, R. L.; Dei, A.; Gatteschi, D. *J. Am. Chem. Soc.* **1985**, *107*, 8128.

S0020-1669(97)01493-6 CCC: $15.00
Published on Web 04/24/1998

ladder-type motif is predominant. For example, Shore and co-workers[11] reported on an organometallic infinite chain compound with Fe−CO−Yb linkages, whereby a significant metal−metal interaction between two adjacent chains finally leads to a ladder-type polymer. Thereby, the rungs of the ladder are generated by direct Fe−Yb metal bonds. Furthermore, the research group has prepared polynuclear structures containing divalent lanthanides (Eu, Yb) and transition-metal (Ni, Pt) cyanoates which also adapt the ladder-type motif.[l3] This time, the rungs of the ladder are created by one of the bridging cyano groups. Moreover, Kahn and co-workers[l4] described polynuclear structures consisting of a ladderlike motif, whereby the lanthanide ions are linked through copper−oxamato complexes. Consequently, the sidepieces of these ladder-molecules consist of Ln−Cu(oxamato) units and also the rungs are formed by the bridging Cu(oxamato) complexes.

Now, the present study concentrates on a further bridging ligand system, namely the oxalate ions (oxalate = $C_2O_4^{2-}$). Previously, our laboratory has reported on the use of these bridging oxalate ions for constructing extended, two- (2D) and three-dimensionally (3D) linked transition-metal complexes.[17,18] Thereby, the resulting polymeric structures of these anionic network compounds, honeycomb layers (2D) versus decagon frameworks (3D), definitely depend on the choice of the templating counterions. Furthermore, and quite remarkably, a large variety of transition-metal ions can be incorporated into these kinds of homo- and heterometallic, supramolecular host−guest compounds. Along this line, we aimed to implement the same design strategy while combining molecular $[Cr^{III}(ox)_3]^{3-}$ "building blocks" with the oxophilic, trivalent lanthanide ions, to realize polynuclear 3d−4f coordination solids. As a matter of fact, it is known that the series of the homometallic lanthanide(III) oxalates with stoichiometries such as $[Ln^{III}_2(\mu\text{-ox})_3(H_2O)_x]\cdot nH_2O$ crystallize in the honeycomb-layer structure type.[19] Consequently, on the basis of the structural data of both, the 3d-metal and 4f-metal oxalato complexes, it might be argued that, for the heterometallic 3d−4f compounds, neutral, polymeric framework structures could result, which express a structural connectivity according to the analogous formula $[Ln^{III}Cr^{III}(\mu\text{-ox})_3(H_2O)_x]\cdot nH_2O$. Thereby, it is important to note that the formula would equally well describe a honeycomb-layer structure or also a ladder-type motif, since both structural architectures express the same kind of connectivity around the metal centers (compare Chart 1). Thus, we anticipate that the exact nature of the structure would finally depend on crystal packing effects, since the lanthanide ion centers are known to have a fairly large flexibility in their coordination geometry, which reflects a typical balance between electrostatic and steric demands.

The present study focuses on the structural features of the four polymeric 3d−4f metal oxalato complexes, but we also present results of two analogous compounds, comprising a 1:1 Ln(III):Cr(III) ratio, containing Eu(III) and Tb(III). These latter lanthanide ions are, in general, remarkable ions considering their photophysical properties. In addition, a preliminary discussion of the corresponding magnetic behavior of the four structurally well characterized 3d−4f compounds will be presented.

Chart 1. Comparison of a Bidimensionnal Honeycomb Motif with a One-Dimensional Ladder-Type Structure, Both Expressing the Same Connectivity and Stoichiometry

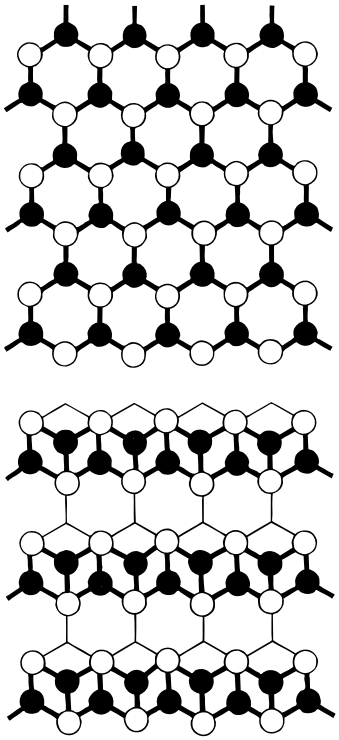

Experimental Section

Materials. All chemicals were of reagent grade and were used as commercially obtained. Standard literature procedures were used to prepare the complexes $K_3[Cr^{III}(C_2O_4)_3]\cdot 3H_2O$ and $(NH_4)_3[Cr^{III}(C_2O_4)_3]\cdot 3H_2O$.[20]

Synthesis. $[La^{III}Cr^{III}(ox)_3(H_2O)_4]_2\cdot 12H_2O$ (1). Single crystals were grown in a test tube with tetramethoxysilane gel containing a 0.05 M $La^{III}(NO_3)_3\cdot 6H_2O$ salt and filled with a layer of 0.05 M aqueous solution of $(NH_4)_3[Cr^{III}(C_2O_4)_3]\cdot 3H_2O$. Within several days, air-stable, dichroic (red−violet), quadratic bipyramidal-shaped single crystals were formed. An X-ray structural analysis was completed. On the basis of the density measurement of single crystals, 12 water molecules of crystallization per formula unit have been assigned.

Microcrystalline samples were obtained by mixing a 0.3 M aqueous solution of $(NH_4)_3[Cr^{III}(C_2O_4)_3]\cdot 3H_2O$ with an equimolar aqueous solution of $La^{III}(NO_3)_3\cdot 6H_2O$. The microcrystalline precipitate was filtered off, washed with water and acetone, and kept in a desiccator over silica gel until constant weight was achieved (7 days). With thermal gravimetry, the water molecules of crystallization for the conditioned, microcrystalline sample were quantitatively determined to give the formula $[La^{III}Cr^{III}(ox)_3(H_2O)_4]_2\cdot 12H_2O$. Anal. Calcd for $C_{12}H_{40}Cr_2La_2O_{44}$: C, 11.35; H, 3.17; Cr, 8.19; La, 21.87. Found: C, 11.70; H, 3.15; Cr, 8.15; La, 22.20. The X-ray powder diffraction data showed this compound to be isostructural to the single-crystal one, and the X-ray powder diffraction data of the calcined compound, after a thermal gravimetric experiment, confirmed the 1:1 La^{III}:Cr^{III} ratio.

$[Ce^{III}Cr^{III}(ox)_3(H_2O)_4]_2\cdot 12H_2O$ (2). Single crystals of this compound were prepared according to the method described above, using a $Ce^{III}(NO_3)_3\cdot 6H_2O$ salt and $(NH_4)_3[Cr^{III}(C_2O_4)_3]\cdot 3H_2O$. An X-ray structural analysis was completed. On the basis of the density measurement of single crystals, 12 water molecules of crystallization per formula unit have been assigned.

The microcrystalline form was prepared according to the method described above. With thermal gravimetry, the water molecules of crystallization for the conditioned, microcrystalline sample were

(17) Decurtins, S.; Schmalle, H. W.; Pellaux, R.; Schneuwly, P.; Hauser, A. *Inorg. Chem.* **1996**, *35*, 1451.
(18) Pellaux, R.; Schmalle, H. W.; Huber, R.; Fischer, P.; Hauss, T.; Ouladdiaf, B.; Decurtins, S. *Inorg. Chem.* **1997**, *36*, 2301.
(19) Birnbaum, E. R. In *Gmelin Handbook of Inorganic Chemistry;* Moeller, T., Schleitzer, E., Eds.; Springer-Verlag: Berlin, 1984; Vol. 39 (D5), p 112.
(20) Bailar, J. C.; Jones, E. M. In *Inorganic Synthesis;* Booth, H. S., Ed.; McGraw-Hill: New York, 1939; Vol. 1, p 35.

Table 1. Crystallographic Data for Compounds **1** and **2**[a]

	1	**2**
formula	$C_{12}H_{40}Cr_2La_2O_{44}$	$C_{12}H_{40}Ce_2Cr_2O_{44}$
fw	1270.26	1272.68
space group	*C*2 (No. 5)	*C*2 (No. 5)
a, Å	36.080(8)	36.075(6)
b, Å	10.906(1)	10.887(1)
c, Å	10.935(2)	10.913(2)
α, *β*, *γ*, deg	90, 105.55(1), 90	90, 105.65(1), 90
V, Å^3	4145.3(13)	4127.2(11)
Z	4	4
T, K	296	296
calcd density, g cm^{-3}	2.035	2.048
measd density, g cm^{-3}	2.04	2.05
λ(Mo Kα), Å	0.710 73	0.710 73
μ, cm^{-1}	20.35	28.06
final R_1 and wR_2 indices based on *F* and F^2, $I > 2s(I)$	0.046, 0.114	0.044, 0.1114
final R_1 and wR_2 indices based on *F* and F^2, all data	0.054, 0.125	0.059, 0.124

[a] R_1 factor definition: $R_1 = \sum(||F_o| - |F_c||)/\sum|F_o|$. SHELXL-97 w$R_2$ factor definition: $wR_2 = [\sum w(F_o^2 - F_c^2)^2/\sum w(F_o^2)^2]^{1/2}$. Weighting scheme: $w = 1/[\sigma^2(F_o)^2 + (np)^2 + 0.00p]$, $p = (\max(F_o^2) + 2F_c^2)/3$.

quantitatively determined to give the formula $[Ce^{III}Cr^{III}(ox)_3(H_2O)_4]_2 \cdot 10H_2O$. In contrast to the single-crystal stoichiometry, only 10 water molecules of crystallization per formula unit had to be assigned for this specific microcrystalline phase. Anal. Calcd for $C_{12}H_{36}Cr_2Ce_2O_{42}$: C, 11.66; H, 2.93; Cr, 8.41; Ce, 22.66. Found: C, 11.85; H, 3.00; Cr, 8.70; Ce, 22.55. The X-ray powder diffraction data showed this compound to be isostructural to the single-crystal one, and the X-ray powder diffraction data of the calcined compound, after a thermal gravimetric experiment, confirmed the 1:1 Ce^{III}:Cr^{III} ratio.

$[Pr^{III}Cr^{III}(ox)_3(H_2O)_4]_2 \cdot 7H_2O$ (3) and $[Nd^{III}Cr^{III}(ox)_3(H_2O)_4]_2 \cdot 7H_2O$ (4). These compounds were prepared as microcrystalline precipitates according to the method described above. The thermogravimetric analysis of both conditioned samples revealed seven water molecules of crystallization per formula unit. Anal. Calcd for $C_{12}H_{30}Cr_2Pr_2O_{39}$: C, 12.17; H, 2.55; Cr, 8.78; Pr, 23.80. Found: C, 12.30; H, 2.65; Cr, 9.05; Pr, 23.55. Calcd for $C_{12}H_{30}Cr_2Nd_2O_{39}$: C, 12.10; H, 2.54; Cr, 8.73; Nd, 24.23. Found: C, 12.10; H, 2.65; Cr, 9.65; Nd, 23.30. The X-ray powder diffraction data showed the samples to be isostructural to the compounds **1** and **2**.

In addition, the X-ray powder diffraction data of the isostructural series (La^{III}, Ce^{III}, Pr^{III}, and Nd^{III}) exhibited the expected, characteristic line shifts, reflecting the decreasing radius of the lanthanide ions.

With trivalent lanthanide ions of an electronic configuration $4f^n$, $n \geq 4$, the analogous synthesis in aqueous solution failed, and no heterometallic compound could be obtained. Thus, mixing Ln(III)-containing salts and $[Cr^{III}(C_2O_4)_3]^{3-}$ salts in aqueous solution leads to the very stabile compounds $[Ln^{III}_2(\mu\text{-ox})_3(H_2O)_x] \cdot nH_2O$. However, the use of adapted organic solvents allows us to obtain the bimetallic compounds.

$[Eu^{III}Cr^{III}(ox)_3] \cdot 3(CH_3)_2SO \cdot 2H_2O$ (5). Powder samples were obtained by mixing 3 mmol of $Eu^{III}Cl_3 \cdot 6H_2O$ in a 10 mL DMSO solution with 3 mmol of $K_3[Cr^{III}(C_2O_4)_3] \cdot 3H_2O$ in a 10 mL DMSO solution. A green precipitate immediately occurs, which was filtered off, washed with DMSO, and dried under vacuum. The TG-MS measurements allowed us to determine quantitatively the number of water and organic solvent molecules, which was confirmed by elemental analysis. The proposed formula is $[Eu^{III}Cr^{III}(C_2O_4)_3] \cdot 3(CH_3)_2SO \cdot 2H_2O$. Anal. Calcd for $C_{12}H_{22}S_3Cr_1Eu_1O_{17}$: C, 19.51; H, 2.98; S, 13.01; Cr, 7.05; Eu, 20.60. Found: C, 21.90; H, 2.90; S, 12.85; Cr, 7.50; Eu, 20.35.

However, single-crystal growth experiments, using tetramethoxysilane gels containing a 0.05 M $Eu^{III}Cl_3 \cdot 6H_2O$ salt and filled with a layer of a 0.05 M solution of $K_3[Cr^{III}(C_2O_4)_3] \cdot 3H_2O$ in DMSO, lead to an agglomeration of crystals that were not suitable for structure determination.

$[Tb^{III}Cr^{III}(ox)_3] \cdot 4(CH_3)_2NCHO \cdot H_2O$ (6). Powder samples were obtained by mixing 3 mmol of $Tb^{III}Cl_3 \cdot 6H_2O$ in a 10 mL DMF solution with 3 mmol of $(NH_4)_3[Cr^{III}(C_2O_4)_3] \cdot 3H_2O$ in a 10 mL DMF solution. A green precipitate immediately occurs, which was filtered off, washed with DMF, and dried under vacuum.

The TG-MS measurements allowed us to determine quantitatively the number of water and organic solvent molecules, which was confirmed by elemental analysis. The proposed formula is $[Tb^{III}Cr^{III}(C_2O_4)_3] \cdot 4(CH_3)_2NCHO \cdot H_2O$. Anal. Calcd for $C_{18}H_{30}N_4Cr_1Tb_1O_{17}$: C, 27.56; H, 3.82; N, 7.13; Cr, 6.62; Tb, 20.28. Found: C, 28.40; H, 3.65; N, 6.95; Cr, 7.05; Tb, 19.70.

Single-crystal growth experiments, using tetramethoxysilane gels containing a 0.05 M $Tb^{III}Cl_3 \cdot 6H_2O$ salt and filled with a layer of a 0.05 M solution of $(NH_4)_3[Cr^{III}(C_2O_4)_3] \cdot 3H_2O$ in DMF, failed.

Crystallographic Data Collection and Structure Determination. Selected crystallographic data and structure determination parameters for compounds **1** and **2** are given in Table 1. Unit cell parameters were determined and intensity data were collected by using an Enraf-Nonius CAD-4 diffractometer with graphite-monochromated Mo Kα radiation. Crystal stability was checked by monitoring three standard reflections at intervals of every 3 h for **1** and **2**, with 8.7% and 6.6% loss of standard intensities observed and decay corrections applied for both data sets. Orientation control was performed by measuring three standard reflections every 400 reflections. Intensities were also corrected for Lorentz and polarization effects, and numerical absorption corrections based on six (**1**) and five (**2**) crystal faces were applied.

A dichroic (red−violet) square-pyramidal crystal of **2** with approximate dimensions of 0.31 × 0.14 × 0.13 mm^3 was chosen for the X-ray structure determination. A monoclinic unit cell was determined from 25 indexed reflections in the range $9.7° < \theta < 19.75°$. The number of intensity data measured were 10 635 (including 141 standards, $2\theta_{max}$ was 56°, *hkl* range ±47, 0−14, ±14). Possible space groups were *C*2, *Cm*, and *C*2/*m*. The structure could be solved in space group *C*2 by using a combination of the Patterson interpretation routine in SHELXS-97[21] and difference Fourier calculations during refinement on F^2 with SHELXL-97.[22] After merging, 5253 unique reflections remained for the refinement. The Cr−Ce−oxalate units and the four coordinated water-oxygen atoms at Ce were refined anisotropically. The remaining 12 water-oxygen atoms were refined with isotropic displacement parameters. Two of them were refined with split positions, altogether four positions with occupancies of 0.5. Some of the residual electron density peaks from difference Fourier calculations were assigned as 12 hydrogen atomic positions. Their coordinates were fixed with fixed isotropic displacement parameters of 0.150 Å^2 in the refinement. The missing 28 hydrogen atomic positions for the asymmetric unit could not be located in the difference Fourier map. The final maximal residual electron density of 3.81 e·Å^{-3} was located 0.79 Å away from Ce(2).

In addition, while having in mind Marsh's review[23] on correct space group choice or Baur and Tillmanns "How To Avoid Unnecessarily

(21) Sheldrick, G. M. *Acta Crystallogr.* **1990**, *A46*, 467.
(22) Sheldrick, G. M. *Program for Crystal Structure Refinement;* University of Göttingen: Göttingen, Germany, 1997.
(23) Marsh, R. *E. Acta Crystallogr.* **1995**, *B51*, 897.

Low Symmetry in Crystal Structure Determination",[24] we tried to find a higher symmetry than C2, in which the structure was solved and refined. Programs MISSYM[25] in PLATON[26] and BUNYIP[27] were used to search for higher symmetry or additional symmetry elements between the two independent structural parts in the asymmetric unit. However, no extra symmetry elements could be detected. But the long *a* axis (36.075 Å) and the similar lengths of ≈10.90 Å for the *b* and *c* axes, and furthermore the observation of apparently systematic reflection conditions in *h*00 with $h = 4n$ (exception: 200), led to a reexamination of the unit cell with LePAGE[28] by extending the default parameters of distances and angle variations. Thereby, it was shown that the transformed unit cell could be tetragonal body centered, with a transformation matrix (001, 010, $\bar{1}0\bar{1}$), leading to new cell parameters of $a = 10.913$ Å, $b = 10.887$ Å, $c = 34.758$ Å, $\alpha = 91.95°$, $\beta = 90°$, and $\gamma = 90°$. A possible space group was $I4_1$ from structural considerations. The deviation of 1.95° from 90° of angle α, the intensity distribution with a merging *R* in space group $I4_1$ of about 40%, and, more important, the fact that no chemical meaningful model could be interpreted from Patterson solutions using idealized tetragonal cell parameters $a = b$ and $\alpha = \beta = \gamma = 90°$ led finally to the conclusion that the higher symmetry was not correct. Thus, we can consider the presented structure as pseudotetragonal, successfully refined in space group *C*2 ($R_{merge} = 3.7\%$), with two independent $[Ce^{III}Cr^{III}(ox)_3(H_2O)_4]$ units.

A dichroic (red−violet), capped square-pyramidal crystal of **1** with approximate dimensions of 0.45 × 0.26 × 0.22 mm^3 was selected for the X-ray structure determination. A monoclinc cell was determined by least-squares refinement of the θ angles of 25 reflections in the interval $11.2° < \theta < 16.7°$. The number of intensity data collected were 12 789 (including 135 standards). After merging, 12 072 unique reflections remained for the refinement, whereby the isostructural model derived from the refinement result of compound **2** was used only by replacing Ce by La atoms. The refinement was similarly performed as for **2**. In accordance with the larger crystal, more significant data could be used (11 243, $I > 2\,\sigma(I)$). Therefore, of the 12 noncoordinated water-oxygen atoms, 6 were refined anisotropically and the remaining 6 isotropically. Two of the latter were split with fixed occupancies of 0.50 for each split position. A total of 30 hydrogen atomic positions were located in the difference electron density map, and they were fixed with fixed isotropic displacement parameters. A total of 10 hydrogen atomic positions could not be found. The final maximal residual electron density of 4.82 e·Å^{-3} was located 0.79 Å away from La(2).

Thermogravimetric Measurements. The thermal decomposition of the powdered polycrystalline samples was followed by a Perkin-Elmer TAS7 thermobalance in a stream (30 mL/min) of synthetic air (80% N_2, 20% O_2). The calcined final product was characterized by powder X-ray diffraction on a Enraf-Nonius Guinier IV-de Wolff FR 552 camera in order to check out the proposed formula.

Magnetic Measurements. Magnetic susceptibility data of the powdered samples were collected with a MPMS Quantum Design SQUID magnetometer in the temperature range of 300−1.8 K at a field of 1000 G. The sample holder was a quartz tube. The output data were corrected for the experimentally determined diamagnetism of the sample holder and the diamagnetism of the samples calculated from Pascal's constants.

Results and Discussion

Description of the Structures. Compound **2** is chosen to represent the isostructural series (La to Nd) for a detailed structural discussion, and therefore, compound **1** needs only to be described briefly in this paragraph. Typically, these heterometallic complexes form a polymeric structure of infinite molecular chains exhibiting a ladder-type motif. Thereby, the solid-state arrangement consists of two almost identical but symmetrically independent types of infinite ladder-molecules.

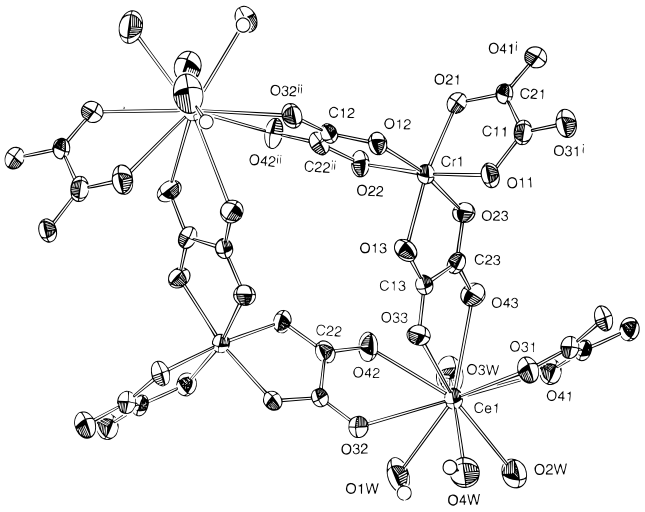

Figure 1. ORTEP drawing (50% probability level) with the labeling scheme of a segment of the extended ladder molecule exhibiting the Cr(1) and Ce(1) coordination of compound **2**. Only the refined hydrogen positions are shown.

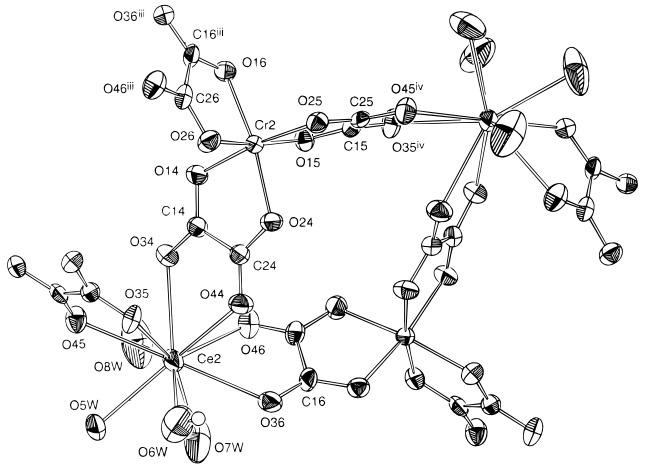

Figure 2. ORTEP drawing (50% probability level) with the labeling scheme of a segment of the extended ladder molecule exhibiting the Cr(2) and Ce(2) coordination of compound **2**. Only the refined hydrogen positions are shown.

$[Ce^{III}Cr^{III}(ox)_3(H_2O)_4]_2 \cdot 12H_2O$ (2). In compound **2**, one of these two types of the heterometallic, infinite molecular chains is assigned with the atomic labels Cr(1) and Ce(1), which distinguishes it from the second type with the labels Cr(2) and Ce(2). The asymmetric unit and the atomic numbering schemes of both independent ladder segments of **2** are shown in Figures 1 and 2, whereas Tables 2 and 3 summarize the atomic fractional coordinates and selected bond lengths and angles for **2**.

The ladderlike structural motif of these polymeric strings is clearly illustrated in Figure 3. Each metal ion in this molecular, heterometallic assembly is alternately linked by three oxalate ligands to three neighboring metal ions (Cr to Ce and vice versa). Thus, the sidepieces and the rungs of the ladder are formed by the oxalate bridges, and moreover, it is interesting to note that the connectivity pattern bears an analogy to that of a heterometallic 2D honeycomb layer structure (compare Chart 1). Within the infinite ladder molecule, each Cr atom is surrounded by six oxygen atoms from the three oxalate ligands. Although there is no crystallographically imposed symmetry at the Cr

(24) Baur, W. H.; Tillmanns, E. *Acta Crystallogr.* **1986**, *B42*, 95.
(25) Le Page, Y. *J. Appl. Crystallogr.* **1988**, *21*, 983.
(26) Spek, A. L. *Acta Crystallogr.* **1990**, *A46*, Suppl. C34.
(27) Hester, J.; Hall, S. BUNYIP. *Xtal 3.5 User's Manual;* Hall, S. R., King, G. S. D., Stewart, J. M., Eds.; University of Western Australia: Lamb, Perth, Australia, 1995.
(28) Le Page, Y. *J. Appl. Crystallogr.* **1982**, *15*, 255.

Table 2. Fractional Coordinates ($\times 10^4$) and Equivalent Isotropic Displacement Parameters ($Å^2 \times 10^3$) for **2**

	x	*y*	*z*	*U*(eq)[a]/*U*(iso)[b]
Ce(1)	1184(1)	−7(1)	8529(1)	35(1)
Cr(1)	−534(1)	243(1)	7024(1)	23(1)
O(11)	−585(2)	1344(5)	5546(5)	30(1)
O(21)	−914(2)	−763(6)	5806(5)	32(1)
C(11)	−814(2)	889(9)	4520(7)	33(2)
C(21)	−983(2)	−364(8)	4666(7)	29(2)
O(31)	894(2)	1373(7)	6542(6)	42(2)
O(41)	1168(2)	−881(7)	6286(6)	41(2)
O(12)	−901(2)	1214(5)	7693(5)	26(1)
O(22)	−548(2)	−871(5)	8429(5)	31(1)
C(12)	−969(2)	741(8)	8689(7)	26(2)
C(22)	771(2)	−498(8)	10904(7)	30(2)
O(32)	1178(2)	1156(7)	10719(5)	36(1)
O(42)	832(2)	−1030(7)	9980(6)	41(2)
O(13)	−97(2)	1213(6)	8062(5)	32(1)
O(23)	−114(2)	−734(5)	6645(6)	31(1)
C(13)	229(2)	783(8)	8035(7)	28(2)
C(23)	219(2)	−388(7)	7247(7)	27(2)
O(33)	547(2)	1232(6)	8583(6)	36(1)
O(43)	525(2)	−887(6)	7234(6)	37(2)
Ce(2)	1323(1)	5306(1)	3462(1)	40(1)
Cr(2)	3031(1)	5318(1)	5600(1)	24(1)
O(14)	2638(2)	6019(6)	4140(6)	33(1)
O(24)	2572(2)	4593(5)	6011(5)	31(1)
C(14)	2294(2)	5692(8)	4096(8)	28(2)
C(24)	2257(2)	4907(8)	5221(7)	30(2)
O(34)	2003(2)	5972(6)	3270(6)	39(2)
O(44)	1930(2)	4610(6)	5287(6)	36(1)
O(15)	3099(2)	3856(5)	4603(5)	29(1)
O(25)	3372(2)	4410(5)	7004(5)	29(1)
C(15)	3306(2)	3041(7)	5274(8)	27(2)
C(25)	3456(2)	3332(7)	6695(8)	27(2)
O(35)	1612(2)	7022(5)	5092(6)	37(2)
O(45)	1362(2)	7546(6)	2591(6)	39(2)
O(16)	3433(2)	6261(5)	5133(5)	30(1)
O(26)	3029(2)	6737(6)	6714(6)	35(1)
C(16)	1499(2)	2314(7)	4329(8)	29(2)
C(26)	3273(3)	7565(7)	6653(8)	31(2)
O(36)	1292(2)	3135(6)	4524(7)	39(2)
O(46)	1671(2)	3515(6)	2736(6)	43(2)
O(1W)	1748(2)	−516(10)	10468(7)	65(3)
O(2W)	1820(2)	−307(13)	7942(7)	85(4)
O(3W)	1256(3)	−2318(10)	8606(8)	72(3)
O(4W)	1524(3)	1985(10)	8774(8)	71(3)
O(5W)	696(3)	6535(8)	2747(18)	133(7)
O(6W)	1004(3)	5366(11)	5187(11)	97(3)
O(7W)	771(3)	3906(9)	2298(13)	110(5)
O(8W)	1243(4)	5498(11)	1082(10)	104(4)
O(9W)	2044(4)	2805(14)	7496(14)	114(4)[b]
O(10W)	1728(4)	6225(14)	7637(14)	113(4)[b]
O(11W)	2450(6)	4890(2)	10508(19)	191(9)[b]
O(12W)	737(5)	3761(19)	6796(18)	158(7)[b]
O(13W)	2196(5)	7387(18)	11160(18)	152(7)[b]
O(14W)	432(5)	7051(17)	5492(15)	134(5)[b]
O(15W)	364(7)	3680(3)	9850(3)	245(12)[b]
O(16A)	2012(8)	3210(3)	780(3)	108(8)[b,c]
O(16B)	2547(8)	6620(3)	8530(3)	112(9)[b,c]
O(17A)	0	7240(7)	0	260(3)[b,c]
O(17B)	1285(12)	4500(5)	8750(4)	118(15)[b,c]
O(18W)	114(10)	3600(4)	4070(3)	295(16)[b]
O(19W)	−26(9)	5630(4)	2770(3)	304(17)[b]
O(20W)	620(10)	6470(4)	9120(3)	307(17)[b]

[a] *U*(eq) is defined as one-third of the trace of the orthogonalized $\mathbf{U_{ij}}$ tensor. [b] Isotropically refined atoms. [c] Atom split over two positions.

sites, the slightly distorted octahedral coordination sphere of the Cr atoms conforms closely to D_3 symmetry, and in the case of the present single crystal, the Cr(1) centers exhibit the Λ configuration whereas the Cr(2) centers show Δ configuration.

In contrast, the Ce centers adapt a coordination number of 10, again with 6 oxygen atoms from the 3 bridging oxalate ligands and 4 additional oxygen atoms from coordinated water molecules. Interestingly, the Ce atom demonstrates the known flexibility of the lanthanoids in adapting various coordination geometries so that, in the actual molecular structure, the three oxalate ligands and the four water ligands are arranged asymmetrically on opposite sides which finally leads to that distinctive structural pattern.

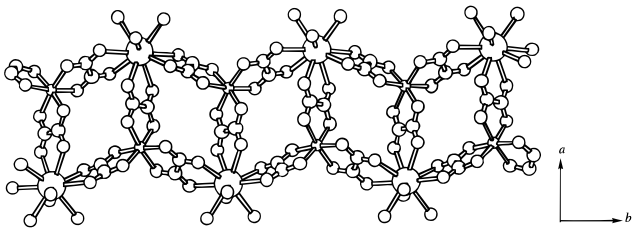

Figure 3. View of a [001] projection of a segment of one extended molecule (Cr(2), Ce(2)) of **2**, accentuating the ladder-type motif. H atoms are omitted.

Table 3. Selected Bond Lengths (Å) and Angles (deg) for **2**

Distances			
Ce(1)−O(4W)	2.470(10)	Ce(2)−O(6W)	2.459(9)
Ce(1)−O(3W)	2.528(11)	Ce(2)−O(8W)	2.544(11)
Ce(1)−O(42)	2.539(7)	Ce(2)−O(46)	2.557(7)
Ce(1)−O(2W)	2.565(8)	Ce(2)−O(7W)	2.559(9)
Ce(1)−O(1W)	2.570(7)	Ce(2)−O(5W)	2.563(9)
Ce(1)−O(43)	2.597(6)	Ce(2)−O(35)	2.595(6)
Ce(1)−O(31)	2.613(7)	Ce(2)−O(34)	2.620(6)
Ce(1)−O(41)	2.612(7)	Ce(2)−O(45)	2.634(7)
Ce(1)−O(33)	2.678(6)	Ce(2)−O(44)	2.641(6)
Ce(1)−O(32)	2.710(6)	Ce(2)−O(36)	2.648(7)
Cr(1)−O(21)	1.966(6)	Cr(2)−O(16)	1.954(6)
Cr(1)−O(22)	1.966(6)	Cr(2)−O(25)	1.955(6)
Cr(1)−O(11)	1.978(6)	Cr(2)−O(26)	1.967(6)
Cr(1)−O(13)	1.980(6)	Cr(2)−O(14)	1.977(6)
Cr(1)−O(12)	1.982(6)	Cr(2)−O(15)	1.982(6)
Cr(1)−O(23)	1.983(6)	Cr(2)−O(24)	1.989(6)
Angles			
O(31)−Ce(1)−O(41)	61.9(2)	O(34)−Ce(2)−O(44)	62.4(2)
O(32)−Ce(1)−O(42)	62.0(2)	O(35)−Ce(2)−O(45)	62.0(2)
O(33)−Ce(1)−O(43)	62.2(2)	O(36)−Ce(2)−O(46)	62.4(2)
O(11)−Cr(1)−O(21)	83.8(2)	O(14)−Cr(2)−O(24)	83.0(2)
O(12)−Cr(1)−O(22)	83.2(2)	O(15)−Cr(2)−O(25)	83.0(2)
O(13)−Cr(1)−O(23)	82.6(2)	O(16)−Cr(2)−O(26)	82.8(3)

The 12 Cr(1)−O and Cr(2)−O distances which vary from 1.954(6) to 1.989(6) Å (average 1.974(6) Å) may be compared with those in the 3D, extended oxalato-bridged $[Na^{I}Cr^{III}(ox)_3]_n^{2n-}$ complex (average 1.960(4) Å)[17] and the analogous $[Li^{I}Cr^{III}(ox)_3]_n^{2n-}$ complex (average 1.977(2) Å).[29] The 12 bond distances Ce(1)−O(oxalate) and Ce(2)−O(oxalate) vary between 2.539(7) and 2.710(6) Å (average 2.621(7) Å); thus they are essentially the same as in the homometallic $[Ce^{III}_2(ox)_3]\cdot 10.5H_2O$ complexes (2.48−2.66 Å, average 2.54 Å).[19] The eight bond lengths Ce(1)−O(coordinated H_2O) and Ce(2)−O(coordinated H_2O) range from 2.459(9) to 2.570(7) Å (average 2.532(7) Å), which again compares well with the average value of 2.57 Å for the homometallic Ce compound.[19] All the bridging oxalate ligands are virtually planar, and they display bond distances and angles within normal limits (see the Supporting Information). Interestingly, the bite angle of the chelating oxalates decreases from an average value of 83.2 to 62.2° in passing from Cr to Ce which is of course in accordance with the increase of the metal to ligand bond distance. The

(29) Decurtins, S.; Schmalle, H. W.; Schneuwly, P.; Ensling, J.; Gütlich, P. *J. Am. Chem. Soc.* **1994**, *116*, 9521.

Table 4. Selected Bond Lengths (Å) and Angles (deg) for **1**

		Distances	
La(1)−O(4W)	2.511(6)	La(2)−O(6W)	2.497(6)
La(1)−O(3W)	2.565(6)	La(2)−O(5W)	2.569(5)
La(1)−O(42)^{i}	2.575(4)	La(2)−O(8W)	2.581(6)
La(1)−O(1W)	2.585(4)	La(2)−O(46)	2.581(4)
La(1)−O(2W)	2.605(5)	La(2)−O(7W)	2.584(5)
La(1)−O(43)	2.622(3)	La(2)−O(35)^{iii}	2.628(3)
La(1)−O(41)^{ii}	2.631(3)	La(2)−O(34)	2.640(4)
La(1)−O(31)^{ii}	2.638(3)	La(2)−O(45)^{iii}	2.641(3)
La(1)−O(33)	2.702(3)	La(2)−O(36)	2.662(4)
La(1)−O(32)^{i}	2.709(3)	La(2)−O(44)	2.673(3)
Cr(1)−O(21)	1.969(3)	Cr(2)−O(25)	1.960(3)
Cr(1)−O(11)	1.971(3)	Cr(2)−O(16)^{iii}	1.964(3)
Cr(1)−O(22)	1.971(3)	Cr(2)−O(26)^{iii}	1.971(3)
Cr(1)−O(23)	1.974(3)	Cr(2)−O(14)	1.971(3)
Cr(1)−O(12)	1.976(3)	Cr(2)−O(15)	1.982(3)
Cr(1)−O(13)	1.983(3)	Cr(2)−O(24)	1.984(3)
		Angles	
O(31)^{ii}−La(1)−O(41)^{ii}	61.62(11)	O(34)−La(2)−O(44)	62.30(10)
O(32)^{i}−La(1)−O(42)^{i}	62.27(10)	O(35)^{iii}−La(2)−O(45)^{iii}	61.93(10)
O(33)−La(1)−O(43)	61.97(10)	O(36)−La(2)−O(46)	62.52(12)
O(11)−Cr(1)−O(21)	83.80(13)	O(14)−Cr(2)−O(24)	82.89(13)
O(12)−Cr(1)−O(22)	82.88(12)	O(15)−Cr(2)−O(25)	82.89(12)
O(13)−Cr(1)−O(23)	82.56(13)	O(16)^{iii}−Cr(2)−O(26)^{iii}	83.17(14)

[a] Symmetry transformations used to generate equivalent atoms: (i) $-x, y, -z+1$; (ii) $-x, y, -z+2$; (iii) $-x+{}^1/_2, y-{}^1/_2, -z+1$.

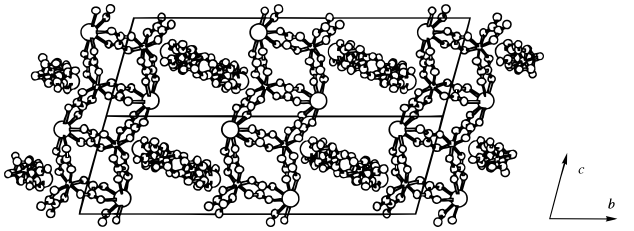

Figure 4. A [100] projection, exhibiting the crystal packing motif of **2**. All water molecules are omitted for clarity.

intrachain Cr(1)−Ce(1) and Cr(2)−Ce(2) distances show an average value of 5.93 Å.

Figure 4 exhibits the regular crystal packing arrangement in the [100] projection. In addition, this solid-state structure type is solvent stabilized with 12 water molecules of crystallization in case of the single-crystal compound **2**.

$[La^{III}Cr^{III}(ox)_3(H_2O)_4]_2\cdot 12H_2O$ (1). This compound is isostructural to the above-described compound **2**. Table 4 summarizes some selected bond lengths and angles for **1**, while the atomic fractional coordinates have been supplied as Supporting Information.

The La coordination is analogous to that of the Ce atom. The 12 bond distances La(1)−O(oxalate) and La(2)−O(oxalate) vary between 2.575(4) and 2.709(3) Å (average 2.642(4) Å); thus, they are essentially the same as in the homometallic $[La^{III}_2(ox)_3]\cdot 10.5H_2O$ complexes (2.49−2.59 Å, average 2.54 Å).[19] The eight bond lengths La(1)−O (coordinated H_2O) and La(2)−O (coordinated H_2O) range from 2.497(6) to 2.605(5) Å (average 2.563(6) Å), which compares well with the average value of 2.54 Å for the homometallic La compound.[19]

Magnetic Properties. The temperature dependences of the magnetic susceptibility for compounds **1**−**4** were measured in the temperature range 1.8−300 K, with an applied field of 1000 G. The plots of $\chi_M T$ versus T for these four compounds are shown in Figure 5. χ_M is the molar magnetic susceptibility corrected for the diamagnetic contribution, and T is the temperature. At high temperatures ($T > 200$ K), the $\chi_M T$ values are essentially constant and they may be compared with the calculated values using the eq 1, which is based on the free-ion

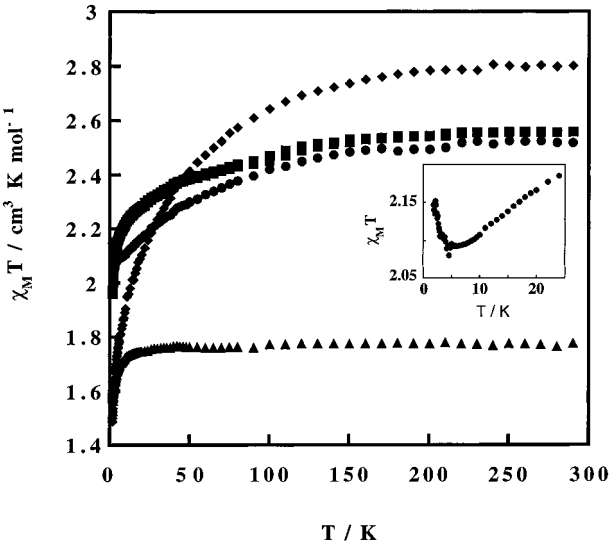

Figure 5. Experimental $\chi_M T$ versus T curves for compounds **1**−**4** (▲ = La (**1**), ■ = Ce (**2**), ◆ = Pr (**3**), ● = Nd (**4**)) in an applied field of 1000 Oe. The insert shows a minimum of $\chi_M T$ at 5 K for compound **4**.

$$\chi_M T = \frac{N_A \beta^2}{3k}\left(g_{Cr^{III}}{}^2 S_{Cr^{III}}(S_{Cr^{III}}+1) + g_{J\,Ln^{III}}{}^2 J_{Ln^{III}}(J_{Ln^{III}}+1)\right) \quad (1)$$

approximation for the lanthanide ions and on the assumption of noncorrelated spin centers, where N_A is the Avogadro number, β the Bohr magneton and k the Boltzmann constant. The g-factor, $g_{Cr^{III}}$, is taken equal to 2, and $g_{J\,Ln^{III}}$ takes the values according to the literature.[30]

The calculated and observed values ($T = 280$ K) for $\chi_M T$ are given in Table 5. Obviously, for compound **1**, $\chi_M T$ is equal to the expected value originating only from uncorrelated spins ($S = {}^3/_2$) of the Cr^{III} ions. Further, while $\chi_M T$ for compound **2** shows also a correspondence between theoretical and experi-

(30) Kahn, O. *Molecular Magnetism*; VCH Publishers: Weinheim, Germany, 1993; p 47.

Table 5. Calculated and Observed Values of the Product of the Molar Magnetic Susceptibility χ_M and the Temperature for Compounds **1**−**4**

compd Ln−Cr	$\chi_M T$ calcd (280 K)	$\chi_M T$ obsd (280 K)
1 (La^{III})	1.87	1.77
2 (Ce^{III})	2.68	2.55
3 (Pr^{III})	3.47	2.80
4 (Nd^{III})	3.51	2.52

mental values, the observed magnetic moments for compounds **3** and **4** are significantly below the calculated ones. However, there are many cases known from the literature where Pr^{III} and Nd^{III} complexes exhibit magnetic moments which are fairly low compared to the expected ones calculated from the free-ion ground terms.[31]

As the temperature is lowered, from 200 to 1.8 K, χ_MT for compounds **2**−**4** decreases, which indicates that an antiferromagnetic interaction takes place between the neighboring paramagnetic centers. In addition, the decrease of the $\chi_M T$ product for compound **1** on cooling to low temperatures points also to the expected effect from a zero-field splitting of the Cr^{III} ions.

Generally, the antiferromagnetic type of interactions between adjacent spins, where $S_A \neq S_B$, leads finally to a ferrimagnetic behavior, and interestingly, in case of compound **4**, there is a clear minimum for the $\chi_M T$ curve at $T = 5$ K. Such a minimum in the $\chi_M T$ product at a finite temperature is known as a signature of a ferrimagnetic system.[30] At the present state, a more detailed rationalization of the magnetic behavior for these ladderlike chain compounds comprising 3d and 4f metal ions is beyond the scope of our report.

Concluding Remarks

We have attempted to present a careful synthetic and structural study in the exciting field of polymeric, heterometallic coordination compounds comprising the transition-metal and rare-earth elements. Now, since most of the structurally characterized, extended 3d−4f coordination compounds reported so far rely on Cu^{II} for the transition-metal site, the herein presented Ln^{III}−Cr^{III} stoichiometries will bring about a substantial extension to the literature data. Thereby, the isostructural series of bimetallic, Ln^{III} = La, Ce, Pr, Nd, and Cr^{III}, oxalate-bridged polymeric compounds reveals a very distinct ladder-type structural motif. However, in accordance with the experience that the crystal structures of the rare-earth-element compounds often change along the lanthanide series, the actual isostructural series could not yet be extended beyond the neodymium ion. Therefore, further experiments are needed for a detailed characterization of the analogous compounds, comprising for instance the europium and terbium ions; such stoichiometries would clearly be of interest for photophysical investigations.

The preliminary study of the magnetic exchange interaction between the paramagnetic centers of the extended ladder-type chain molecules reveals the occurrence of an antiferromagnetic-type interaction. However, a more detailed discussion based on a model calculation for a Ln^{III}−Cr^{III} system with a ladder-type structure will certainly need special attention in a more theoretical study.

Acknowledgment. Gratitude is expressed to the Swiss National Science Foundation for financial support under Project No. 20-45750.95.

Supporting Information Available: A complete table of crystal data and structure determination parameters for **1** and **2**, tables of fractional coordinates and equivalent isotropic displacement parameters for **1**, bond lengths and angles for **1**, and bond lengths and angles for **2**, and a figure of **2**, exhibiting the crystal packing motif ([001] projection) (13 pages). Ordering information is given on any current masthead page.

IC971493K

(31) Boudreaux, E. A.; Mulay, L. N. *Therory and Application of Molecular Paramagnetism*; J. Wiley & Sons: New York, 1976; p 271.